Mechanisms of Temporary Inhibition in *Streptomyces* Subtilisin Inhibitor Induced by an Amino Acid Substitution, Tryptophan 86 Replaced by Histidine†

Atsuo Tamura,‡ Kenji Kanaori,‡ Shuichi Kojima,§ Izumi Kumagai,§ Kin-ichiro Miura,§ and Kazuyuki Akasaka*,‡

Department of Chemistry, Faculty of Science, Kyoto University, Kyoto 606, Japan, and Department of Industrial Chemistry, Faculty of Engineering, University of Tokyo, Tokyo 113, Japan

Received September 7, 1990; Revised Manuscript Received January 3, 1991

ABSTRACT: Just one amino acid substitution (Trp86 replaced by His), which is more than 30 Å away from the reactive site, changed the inhibitor, *Streptomyces* subtilisin inhibitor (SSI), into a temporary inhibitor without a change in the inhibition constant. When the inhibitor was in excess of subtilisin BPN′, the wild-type SSI was stable under protease attack, while the mutant inhibitor was hydrolyzed to peptide fragments in an all-or-none manner. The mechanism of this temporary inhibition induced by the amino acid substitution was studied on the basis of structural, thermodynamic, and kinetic data obtained by a combined use of NMR, hydrogen–deuterium exchange, differential scanning calorimetry, and gel filtration HPLC. The mutation did not induce major structural changes, and in particular, the structure of the enzyme-binding region was virtually unaffected. The denaturation temperature of SSI, however, was decreased by 10 deg upon mutation, although it still remained a thermostable protein with a denaturation temperature of 73 °C. Furthermore, the activation enthalpy for denaturation was reduced dramatically, to half that of the wild type. When the mutated SSI is present in excess of the enzyme, the proteolysis followed first-order reaction kinetics with respect to the total concentration of the mutated SSI molecules present. From these combined results, we conclude that the proteolysis proceeds not through the native form of the inhibitor in the inhibitor–enzyme complex but through the denatured (unfolded) form of the inhibitor whose fraction is increased by the mutation. This conclusion states that the necessary condition for being a serine protease inhibitor lies not only in the design of the reactive site structure that is highly resistant to protease attack but also in the suppression of such structural fluctuation that brings about cooperative denaturation. In contrast, when the protease existed in excess of the mutated inhibitor, the proteolysis reaction was accelerated by more than 2 orders of magnitude. Furthermore, the reaction occurred even in the wild-type SSI at a comparable rate as in the mutated protein. This indicates that in the enzyme excess case another, more efficient digestion mechanism involving fluctuation within the native manifold of the inhibitor dominates.

A protein protease inhibitor exists as a paradox in the sense that it is a protein and binds tightly to the reactive site of the target enzyme and yet is not hydrolyzed by the protease. However, some perturbations may change an inhibitor into a substrate with a temporary inhibition, as in the case of reduced bovine pancreatic trypsin inhibitor (BPTI;[1] Kress et al., 1968), reconstituted soybean trypsin inhibitor (Koide et al., 1974), and active fragments of soybean inhibitor (Odani & Ikenaka, 1978). More recently, it was reported that some BPTIs, obtained by a combination of random mutagenesis and disulfide reduction, became trypsin substrates (Coplen et al., 1990). In the case of *Streptomyces* subtilisin inhibitor (SSI), which is a serine protease inhibitor produced by *Streptomyces albogriseolus* and inhibits subtilisin BPN′ and other proteases of various origins (Hiromi et al., 1985), removal of the C-terminal four residues by carboxypeptidase A resulted in temporary inhibition (Sakai et al., 1980). However, the mechanism of this temporary inhibition has not yet been made clear.

In the present study, just one amino acid replacement by site-directed mutagenesis, i.e, Trp86 replaced by His (hereafter abbreviated to W86H) at a site some 30 Å from the reactive site (Met73-Val74), was found to change SSI into a temporary inhibitor. Several other cases of single amino acid replacement in regions remote from the reactive site also resulted in the similar temporary inhibition in SSI (Kojima et al., to be

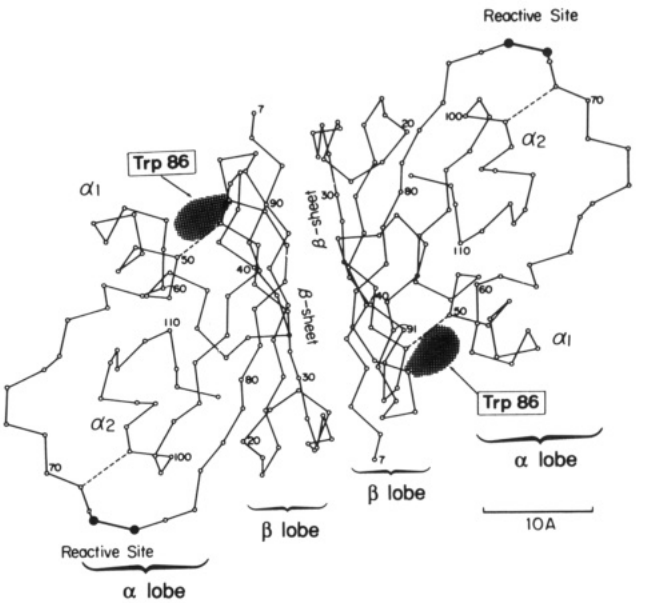

FIGURE 1: Three-dimensional structure of *Streptomyces* subtilisin inhibitor (SSI) determined by X-ray analysis (Mitsui et al., 1979a). The broken lines represent disulfide bridges. The subunit may be divided into two structural regions, the β lobe mainly consisting of five-stranded β-sheet and the α lobe mainly consisting of two α-helices (α_1 and α_2) and the reactive site segment. The Trp86 ring on the β_4-strand fills the cleft between the two lobes.

† This work was supported by a Grant-in-Aid for Scientific Research from the Ministry of Education, Science and Culture of Japan and by CIBA GEIGY Foundation for the Promotion of Science.

‡ Kyoto University.

§ University of Tokyo.

0006-2960/91/0430-5275$02.50/0

Table I: Summary of the Parameters Characterizing the Wild-Type SSI and Its Mutant W86H

	inhibn const, K_i[a] (M^{-1})	denaturation temp, T_D in ^1H_2O[b] (°C)	denaturation temp, T_D in ^2H_2O[c] (°C)	enthalpy of denaturation, ΔH[b] (kcal/mol)	rate of unfolding, k_1[d] (min^{-1})	equilibrium const for denaturation, K_d[e]	rate of proteolysis $[I]_{total} > [E]_{total}$[f] ($min^{-1}$)	rate of proteolysis $[E]_{total} > [I]_{total}$[g] ($min^{-1}$)
wild type	$1.8 (\pm 0.3) \times 10^{-11}$	82.8	86.1	146	1.0×10^{-5}	5.0×10^{-10}	$<1 \times 10^{-6}$	1.34×10^{-2}
W86H	$2.7 (\pm 0.9) \times 10^{-11}$	72.7	77.2	126	6.3×10^{-3}	6.0×10^{-7}	1.27×10^{-4}	1.87×10^{-2}

[a] Momma et al. (1990). [b] From differential scanning calorimetry. [c] From proton NMR. [d] From the hydrogen–deuterium exchange experiment at 42 °C in ^2H_2O (pH 9.0). [e] From the hydrogen–deuterium exchange experiment at 42 °C in ^2H_2O (pH 7.0). [f] The first-order rate constant of the proteolysis of the inhibitor at 42 °C obtained by HPLC. [g] The converged value to the first-order rate constant of the proteolysis of the inhibitor at 42 °C obtained by HPLC.

published). Thus, a detailed comparative study between the wild-type SSI and W86H was undertaken using structural, thermodynamic, and kinetic methods, in order to obtain clues to the paradox of the inhibitor and its design.

The three-dimensional structures of SSI (Figure 1; Mitsui et al., 1979a) and of its complex with subtilisin BPN′ (Hirono et al., 1984) have been determined by X-ray crystallography. SSI is a dimeric protein consisting of two identical subunits whose interface is maintained by a five-stranded β-sheet. The subunit may be looked upon as composed of two structural groups, the "β lobe" and the "α lobe", the former consisting of the β-sheet, and the latter consisting of two short α-helices and the reactive site segment (Akasaka et al., 1988). Two disulfide bridges exist, one (Cys71–Cys101) connecting the reactive site segment to the α_2-helix and the other (Cys35–Cys50) linking the α lobe to the β lobe. In the interior part of the protein, the connection between the α and β lobes appears to be maintained only through hydrophobic interactions.

Trp86 apparently fills the gap between the α lobe and β lobe (Figure 1), but the nature of its microenvironment has been a matter of controversy. The solvent accessibility of Trp86 in free (uncomplexed) SSI is 15% by X-ray analysis, but there have been arguments on the extent of its exposure in solution. For example, the Raman spectrum (Harada et al., 1982) and photo-CIDNP (Akasaka et al., 1981) show inaccessibility of the solvent, while studies of solvent perturbation (Inouye et al., 1977), chemical modification (Aoshima, 1976), and fluorescence quenching (Komiyama & Miwa, 1980) show considerable degrees of accessibility. As for the mobility of Trp86, X-ray analysis shows that the *B* factor of the side chain is very small, while deuterium NMR study shows the existence of some mobile components of the side chain in addition to the main fraction, which is held rigidly in the whole protein molecule (Akasaka et al., 1988). Genetically, Trp86 is preserved within the related inhibitors (Hiromi et al., 1985) and the tertiary structure around this position is also maintained (Mitsui et al., 1979b).

His was chosen for replacement of Trp86 for the following reasons. First, it is suited for an evaluation of the role of the hydrophobic interaction at position 86, as there are large differences in free energy of transfer from ethanol to water, i.e., 3.40 and 0.50 kcal/mol (Nozaki & Tanford, 1971), or in the calculated solvation energy, i.e., 2.6 and 0.64 kcal/mol (Eisenberg & McLachlan, 1986), between Trp and His, respectively. Second, information on the solvent accesibility at position Trp86 would be obtained. Third, His gives easily traceable signals in proton NMR measurements.

[1] Abbreviations: SSI, *Streptomyces* subtilisin inhibitor; W86H, a mutated SSI with an amino acid substitution, Trp86 replaced by His; BPTI, bovine pancreatic trypsin inhibitor; NMR, nuclear magnetic resonance; DQF-COSY, double-quantum-filtered correlation spectroscopy; DSC, differential scanning calorimetry; HPLC, high-performance liquid chromatography.

Materials and Methods

Site-Directed Mutagenesis. The SSI gene from *S. albogriseolus* S-3253 had been cloned and expressed in *Streptomyces lividans* 66 as described elsewhere (Obata et al., 1989a,b). The conversion of Trp86 to His was performed by oligonucleotide-directed mutagenesis (Morinaga et al., 1984) using plasmid pSIAX (Kojima et al., 1990) and the mutagenic primer 5′-C GGC GTC C*A*C* CAG GGC A-3′, where asterisks following the residue indicate mismatched bases. The conversion was confirmed by dideoxy sequencing. After the reconstruction of the entire SSI gene, *Sac*I–*Sph*I fragment was inserted into the *Sac*I–*Sph*I of streptomycete plasmid pIJ702 (Katz et al., 1983) as described previously (Kojima et al., 1990). *S. lividans* 66 was transformed by this plasmid.

Purification of SSI. The wild-type SSI was obtained by cultivating *S. albogriseolus* S-3253 in polypepton media as originally proposed (Sato & Murao, 1973). Secreted SSI was precipitated with ammonium sulfate and then purified by passing through an anion-exchange (DE52, Whatman) and a gel filtration (Sephacryl S-200, Pharmacia) column. W86H was obtained in the same manner, except that the transformed *S. lividans* was cultivated in tryptone soya broth medium (OXOID). The amino acid compositions of the wild-type SSI and W86H were confirmed by amino acid analysis.

NMR Measurements. Proton NMR spectra were measured on a JEOL GX-400 spectrometer operating at 400 MHz. The concentration of SSI was 5 mg/mL for one-dimensional NMR measurements and 10 mg/mL for two-dimensional NMR measurements in 0.025 M deuterated phosphate buffer (pH 7.0). The pH values given are the direct readings of the pH meter calibrated against ^1H_2O buffers.

Differential Scanning Calorimetry (DSC). Calorimetric measurements were made in a DASM-4 scanning microcalorimeter. The temperature scanning rate was 1 K/min. The concentration of SSI was 1 mg/mL in the 0.025 M phosphate buffer containing 0.10 M NaCl (pH 7.0).

Gel Filtration HPLC. Gel filtration high-performance liquid chromatography (HPLC) was performed on a TSK G2000SW column (7.5 mm × 60 cm), with elution by 0.10 M phosphate buffer (pH 7.0) at a flow rate of 0.8 mL/min at 10 °C. The concentration of SSI was 2 mg/mL in 0.1 M phosphate buffer, pH 7.0. Aliquots of 10 μL were taken at appropriate intervals and monitored at 280 nm at 10 °C.

Results and Discussion

The Inhibition Constant. The K_i values against subtilisin BPN′ were determined to be 1.8 (±0.3) × 10^{-11} M for the wild-type SSI and 2.7 (±0.9) × 10^{-11} M for W86H (Momma et al., 1990; see Table I). The near coincidence of the two K_i values indicates that the interactions between the active site region of subtilisin BPN′ and the reactive site region of SSI were not changed by the mutation. This would mean that the structure of the enzyme-binding region of SSI was unaltered

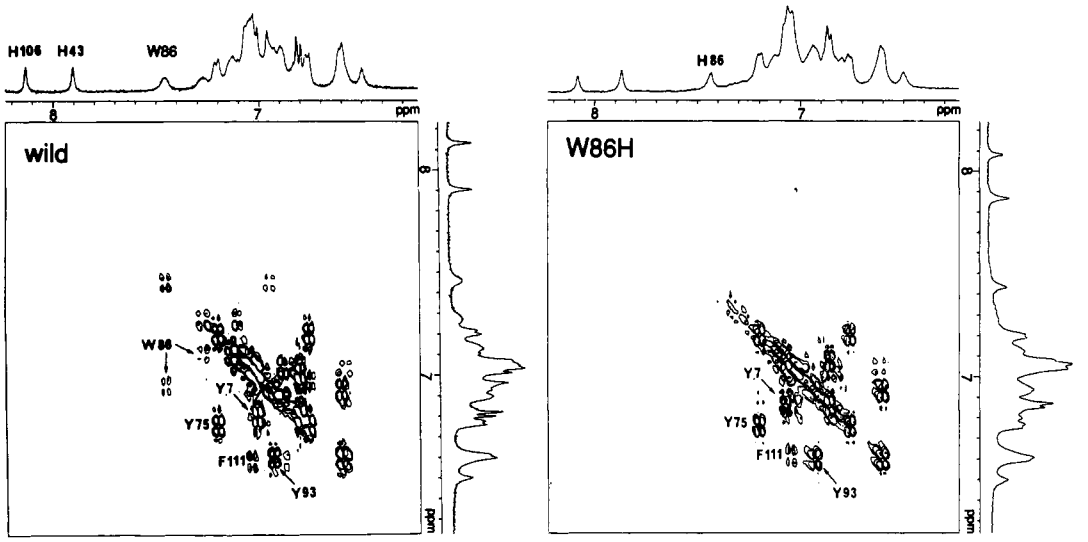

FIGURE 2: Phase-sensitive double-quantum-filtered (DQF) COSY spectra (aromatic region) of the wild-type SSI and W86H (both 10 mg/mL in 0.025 M deuterated phosphate buffer, pH 7.0) at 42 °C. Carrier frequency on the solvent $^1H^2HO$ in the center, $\omega_1 = \omega_2 = 4000$ Hz with data points of 256 and 2048, respectively. After zero filling in the ω_1 dimension, sine bell resolution enhancement with phase shift was applied before Fourier transformation.

by the mutation which occurred 30 Å away from the reactive site.

Structural Changes upon Mutation. The overall appearance of the one-dimensional proton NMR spectrum of W86H was very much similar to that of wild-type SSI, showing that they both have similar tertiary structure. In order to examine more subtle spectral changes induced by the mutation in detail, two-dimensional NMR spectra (phase-sensitive DQF-COSY; Wüthrich, 1986) were measured at 42 °C for the wild-type SSI and W86H (Figures 2 and 3). Although, so far, its large molecular weight (23 000) has prevented us from assigning all the proton signals, specific changes in chemical shifts will give us valuable information as to where conformational changes have taken place. Figure 2 (aromatic region) clearly shows the appearance of a new signal of the substituted His C_2 proton of W86H in place of that of Trp C4 proton at an exceptionally high field (Gross & Kalbitzer, 1988) indicative of the diamagnetic shielding effect of the β-sheet. Invariance in the chemical shifts of the ring proton signals of Tyr75 [P2′ site; see Schechter and Berger (1967) for nomenclature] and of Tyr93 (which protrudes into the hydrophobic core from the β-sheet) indicates that no conformational changes occurred in the vicinity of Tyr75 of the reactive site segment and of Tyr93 of the hydrophobic core. The change in the chemical shifts of Tyr7, which is in the neighboring β-strand and 10 Å away from Trp86, may suggest some structural changes around the N-terminal region. The slight change in the chemical shifts of Phe111, located within 5 Å of His106, is caused by the difference in degree of protonation of His106 between the wild-type SSI and W86H at pH 7.0 (cf. Figure 4). In Figure 3 (aliphatic region), no chemical shift changes were detected in the methyl proton signals of three Met residues which are located at the P1 site (Met73), at the P4 site (Met70), and in the hydrophobic core (Met103 in the middle of the α_2 helix). Many of the methyl proton signals of Leu and Val remained unchanged, but some showed dramatic changes in chemical shifts. One of these is the methyl proton signal of Leu12, which was high field shifted to 0.13 ppm in the wild type by the direct effect of the ring current of Trp86, is now missing in W86H. There were also changes in chemical shifts of several Ala and Thr residues. Some of these may be caused directly by the loss of the ring current effect of Trp86 (Ala11 and Thr10 in the neighboring β-strand). A new signal appeared at 1.47 ppm which is attributable to the methyl residue of Ala of the extra three amino acid residues (Ala-Pro-Gly) at the N-terminal in this expression system (Obata et al., 1989b). Some small (within 0.1 ppm) changes of the methyl proton signals, however, may reflect conformational changes upon mutation. The ϵ-proton signal of Lys89 located relatively close (about 10 Å) to Trp86 showed some change. The peptide NH proton signals which do not disappear in ^2H_2O are assignable to those in the β-sheet from the similarity to their chemical shifts to those of the wild-type SSI (Akasaka et al., 1985). The similarities of their shifts, except those of Leu12 and Leu33 near Trp86, suggest that the β-sheet structure remains largely unaffected (cf. Figure 7). The assignments of the NH proton signals of Leu were made on the basis of those of the α-protons (Westler et al., 1988).

In order to detect structural changes in a wider pH range, the effects of pH on the proton NMR spectra were examined (Figure 4 for His C_2 protons). The apparent pK_a value of His106 was decreased by 0.19 unit (from 6.40 to 6.21) by the mutation. This indicates that changes in distances took place between His106 and neighboring charged amino acid residue(s), attributed to a small conformational change around His106, which is located at the end of the α_2-helix. The direction of the pK_a shift suggested that either a positive charge (Arg95 or Arg65; Fujii et al., 1980) moved closer to His106 or a negative charge (Glu102) moved away from His106. His43 was not titratable in either protein, but showed small but distinct chemical shift change upon mutation. This indicates that a slight conformational change also occurred at His43 which is located in the hinge region connecting the α and β lobes. The imidazole ring of His86 was not titratable in the native conformation, showing that the solvent water was not easily accessible to His86 in the native conformation. The transition pH for acid denaturation of SSI increased by as much as 1.5 pH unit (from 3.0 to 4.5) by the mutation, indicating that the protonation of His86 is a decisive factor for acid denaturation of W86H. The pK_a's for three Tyr (7, 75, and 93) were the same as those of the wild-type SSI (11.0, 11.8, and 12.6, respectively; Fujii et al., 1981), indicating that the charge interactions between these Tyr and other charged groups were not affected by the mutation.

With all the information obtained above, we may conclude that, although there are indications of subtle conformational

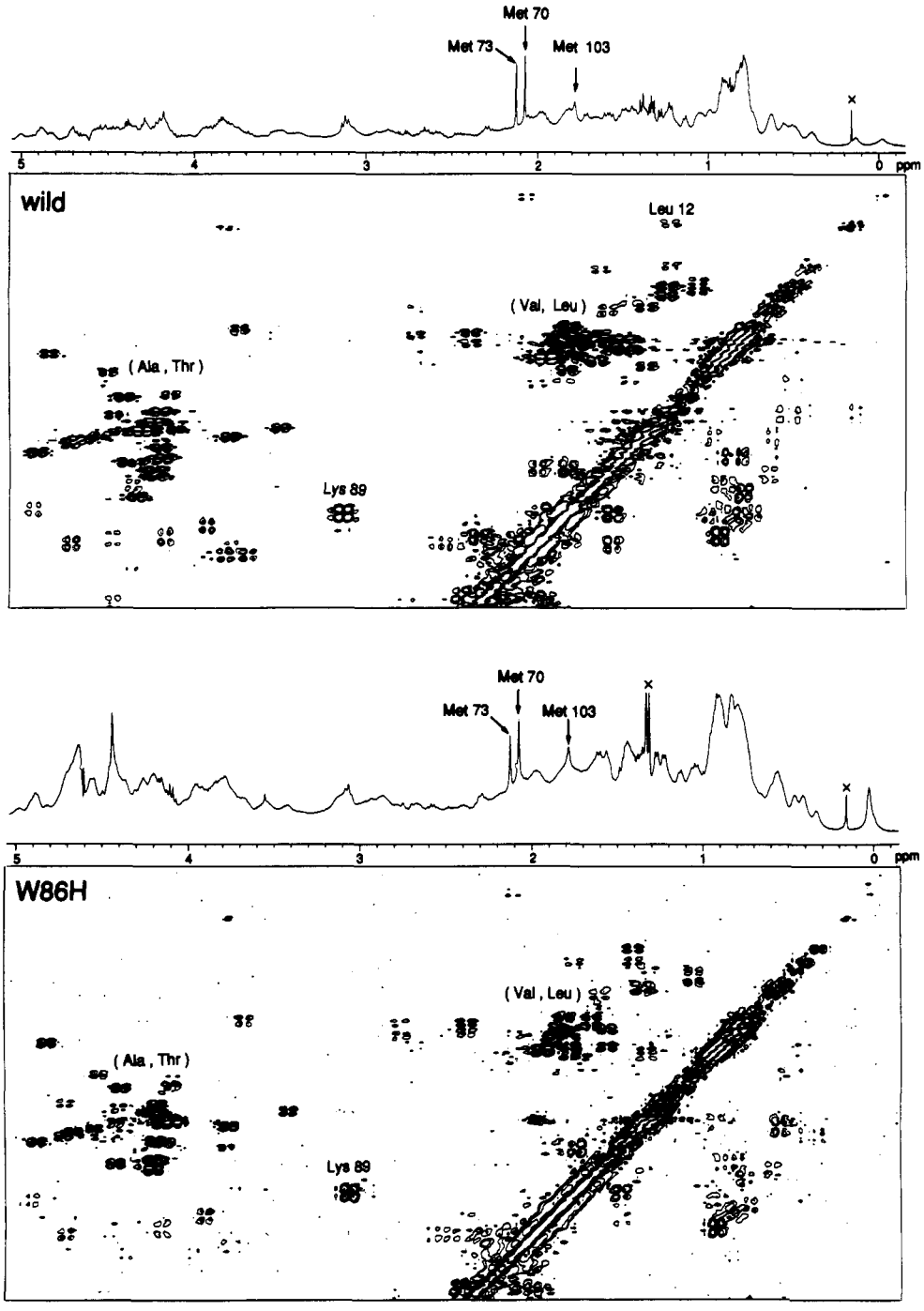

FIGURE 3: Phase-sensitive DQF-COSY spectra (aliphatic region) of the wild-type SSI and W86H. The experimental conditions were the same as in Figure 2.

changes induced by the mutation at various regions of the core, distinct changes are confined to the region of the β-sheet (β_1-, β_4-, and β_5-strands) within about 10 Å of Trp86. Especially, we emphasize the point that no indication was obtained for a conformational change in the enzyme-binding region itself.

Thermodynamic Stability. Changes in thermal stability caused by the mutation were studied by differential scanning calorimetry (DSC; Privalov, 1979). Figure 5 shows the DSC curves of the wild-type SSI and W86H in 0.025 M phosphate buffer (^1H_2O), pH 7.0. The transition temperatures for denaturation (T_D), which are regarded here as the peak temperatures of the DSC curve, were 82.8 °C for the wild-type SSI and 72.7 °C for W86H (see Table I). Differences in the van't Hoff enthalpy between the native state (N) and the denatured state (D) were determined to be 146 kcal/mol for the wild-type SSI and 126 kcal/mol for W86H, respectively (see Table I). The results indicate that the enthalpy difference between the N and D states was reduced by about 15% by the mutation. The high enthalpy values indicate that the thermal denaturation observed is a cooperative phenomenon both for the wild-type SSI and W86H.

The thermal stability of W86H was also studied in ^2H_2O at pH 7.0 by using proton NMR (Figure 6). The T_D of W86H, defined as the temperature at which the peaks of the native and denatured proteins have equal intensities, was 77.2 °C. This corresponds very well to the T_D of 73.1 °C in ^1H_2O, in view of the fact that the T_D of SSI is increased by about 4 deg in ^2H_2O as compared to ^1H_2O (Nakanishi & Tsuboi, 1976; Komiyama et al., 1984). The same T_D was obtained in ^2H_2O at pH 9.0 as in the lower part of Figure 6 in which

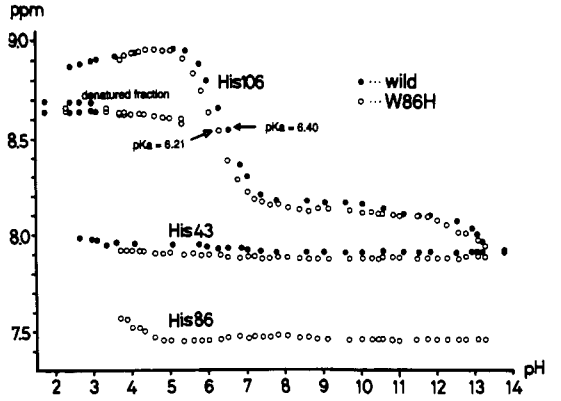

FIGURE 4: Plots of His C_2 proton NMR signals against pH for the wild-type SSI (●) and W86H (○), measured at 25 °C in ^2H_2O environment. The points around 8.65 ppm originate from the acid-denatured form of SSI.

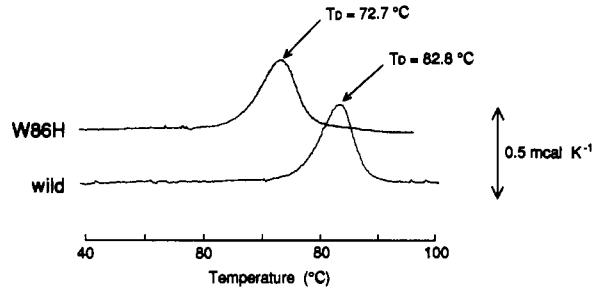

FIGURE 5: Differential scanning calorimetry (DSC) curves for the wild-type SSI and W86H in 0.025 M phosphate buffer (pH 7.0) containing 0.10 M NaCl. Temperature scanning rate was 1 K/min.

spectral changes in the aromatic region are shown around T_D, denying that the positive charge of His affects the decrease in thermostability upon mutation at pH 7.0. Throughout the thermal transition region, the ratios of the individual peak intensities for various amino acid residues between the native and denatured components were the same, and no intermediate signals were detected, as was the case for the wild-type SSI (Kanaori et al., to be published). The results confirmed that the native conformation of the reactive site segment was disrupted simultaneously with the disruption of the hydrophobic core including His86. Thus the thermal denaturation of W86H is represented very well by a phase transition concomitant with the exposure of hydrophobic amino acids to solvent water as has been established for most globular proteins (Privalov & Gill, 1988; Privalov, 1989).

In general, there are two ways to destabilize a protein: one is to destabilize the native state and the other is to stabilize the denatured state. In the present case, the native state must certainly be destabilized because van der Waals interactions must have been reduced by the replacement of Trp with His. It is also probable that the denatured state is stabilized at least to some extent upon mutation, because the almost sequestered character of the residue at position 86 in the native state should result in certain exposure to solvent water in the denatured state and His is more preferable than Trp for this exposure. The fact that the chemical shifts of all three His at positions 43 (in the hydrophobic core region), 106 (in the α_2-helix and solvent accessible), and 86 merged into a nearly identical value of 7.68 ppm (at 77 °C) corresponding to a free His (Figure 6) indicates that the sequestered His86 was fully exposed to the solvent upon heat denaturation.

Structural Fluctuation. Although the major unfolding of the native structure is a rare incident and population of the unfolded fraction is quite small at temperatures more than 30

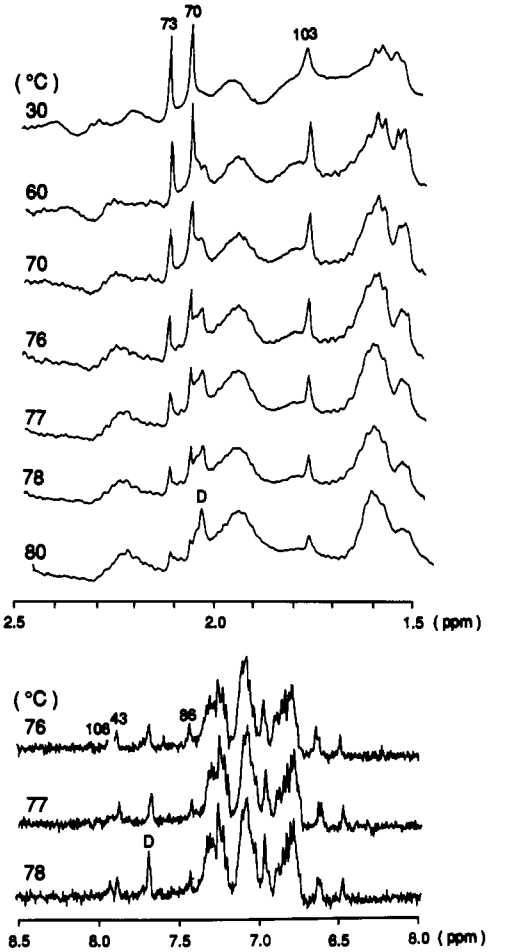

FIGURE 6: Temperature dependence of proton NMR spectra of W86H in the methyl proton region of Met70, 73, and 103 (upper) in 0.10 M deuterated phosphate buffer (pH 7.0), and in the aromatic region (lower) in 0.10 M deuterated borate buffer (pH 9.0). The His C_2 proton signals have been assigned to specific residues (43, 86, and 106) as shown. D represents the denatured fraction.

deg below the T_D, it is possible to measure the rate of unfolding by observing the exchange rate of peptide NH protons in the hydrophobic core region with the deuterons of the solvent ^2H_2O (Tsuboi & Nakanishi, 1979; Woodward et al., 1982). Here the proton NMR spectroscopy was utilized to evaluate the unfolding rate of SSI.

Figure 7 shows the time course of the proton NMR spectra which represents the exchange of NH protons of W86H at 35 °C, pH 9.0. These peptide NH proton signals remained unchanged in ^2H_2O after 3 h at 20 °C at pH 9.0. They were assignable to those in the β-sheet from the similarity of their chemical shift values with the corresponding protons of the wild-type SSI. Upon increasing the temperature above 35 °C, all these signals reduced their intensity almost simultaneously, indicating that the exchange is associated with a cooperative unfolding (Figure 7).

The hydrogen–deuterium exchange reaction of the buried peptide NH protons proceeds in two steps, i.e., the exposure of the peptide NH protons to the solvent ^2H_2O, followed by the exchange of protons with deuterons. When the latter is much faster than the former (EX1 mechanism), the observed hydrogen–deuterium exchange rate reflects directly the rate of exposure, i.e., the rate of unfolding of the protein. One of the criteria for the EX1 mechanism is that overall exchange rate is invariant over a certain range of pH. Figure 8 shows the pH variation of the exchange rate of the peptide NH protons of the wild-type SSI at 54 °C (Akasaka et al., 1985) and of W86H at 35 °C. The exchange rate of W86H reached

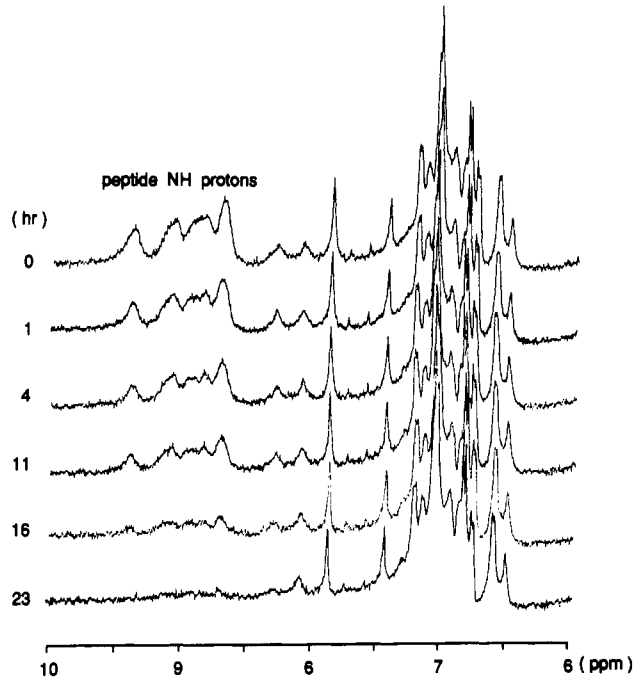

FIGURE 7: Time course of the hydrogen–deuterium exchange reaction of peptide NH protons in W86H in 0.025 M deuterated borate buffer (pH 9.0) at 35 °C, followed by proton NMR at 400 MHz.

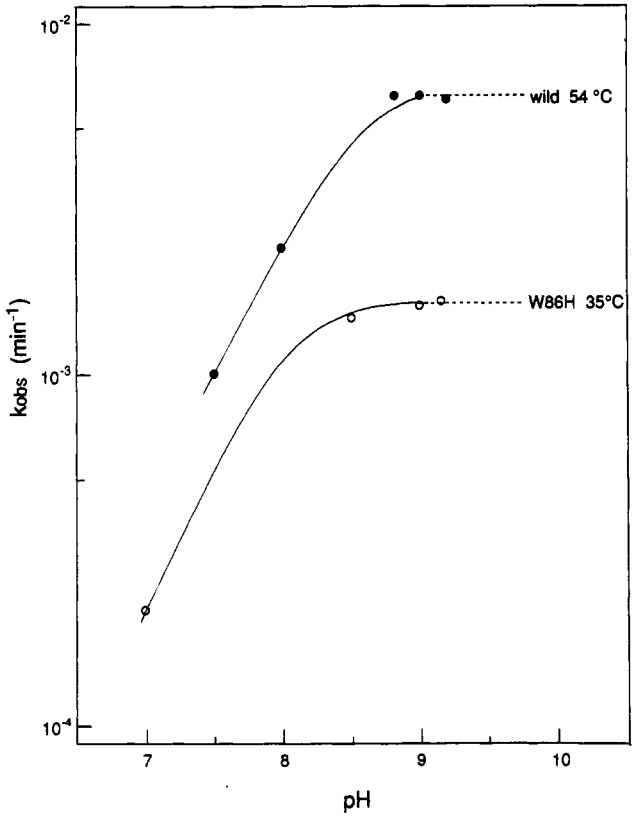

FIGURE 8: pH dependence of the apparent rate constant (k_{obs}) of the hydrogen–deuterium exchange reaction in W86H at 35 °C. For the wild-type SSI, data at 54 °C were adopted from Akasaka et al. (1985).

a plateau at pH above 8.5, suggesting that in this pH range the rate represents the major unfolding rate of W86H as in the case of the wild-type SSI (Akasaka et al., 1985). Thus temperature dependence of the unfolding rate was measured at pH 9.0. Rate constants obtained were $k_1 = 1.84 \times 10^{-4}$ min^{-1} at 30 °C, 1.50×10^{-4} min^{-1} at 35 °C, and 6.31×10^{-3} min^{-1} at 42 °C. The rates were much higher than the corresponding rates of the wild-type SSI. For example, the rate constant of the wild-type SSI, extrapolated to 42 °C, was only $k_1 = 1.0 \times 10^{-5}$ min^{-1}, while $k_1 = 6.31 \times 10^{-3}$ min^{-1} in W86H. This means that in W86H half of the native species turn into the unfolded (denatured) form in every 110 min, while keeping the equilibrium overwhelmingly toward the native fraction. The activation enthalpy for unfolding was estimated from the temperature dependence of the exchange rate to be 35 kcal/mol, which is half that of the wild-type SSI (70 kcal/mol), indicating that the activation enthalpy for unfolding is greatly reduced by the mutation. The reduction of the activation enthalpy of unfolding as much as 35 kcal/mol cannot be attributed to the enthalpic destabilization of the native state alone. A significant lowering of the enthalpy level of the activated state must be involved. This indicates either that the unfolding of W86H bypasses the highest energy barrier existing in the wild-type SSI or that one (or some) of the unfolding steps responsible for the highest energy barrier is modified by the mutation.

Because of the essentially two-state nature of the denaturational transition, as verified in the foregoing section, we may reasonably assume that the unfolded state, in which the hydrogen–deuterium exchange reaction takes place in the most buried region of the β-sheet, is nothing but the denatured state (D) itself. Thus from the hydrogen–deuterium exchange studies at pH 7.0 (under the EX2 mechanism), we can evaluate the equilibrium constants K_D between the native (N) and the denatured (D) states of the inhibitor:

$$K_D = \frac{[D]}{[N]} = \frac{k_1}{k_2} \quad (1)$$

in the reaction

$$N \underset{k_2}{\overset{k_1}{\rightleftharpoons}} D \quad (2)$$

where k_1 and k_2 represent the unfolding and folding rate constants, respectively. The equilibrium constants (K_D) are given as the ratios of the apparent (experimentally observed) hydrogen–deuterium constants (k_{obs}) to the rate constant (k_e) of exchange of the hydrogen atom completely exposed to the solvent ^2H_2O (Hvidt & Nielsen, 1966). By use of the k_{obs} and k_e values at pH 7.0 [$k_e = 1126$ min^{-1} from Takahashi et al. (1978)], the equilibrium constants K_D were determined to be 6.0×10^{-7} for W86H and 5.0×10^{-10} for the wild-type SSI at 42 °C. From eq 1, the folding rate constants (k_2) were then determined to be 1.0×10^4 min^{-1} for W86H and 2.0×10^4 min^{-1} for the wild-type SSI. We note that the two k_2 values are rather close. We may therefore conclude that the large difference in the equilibrium constant K_D between W86H and the wild-type SSI is mainly due to the difference in the unfolding rate k_1.

It is to be noted that the K_D value of the wild-type SSI is extremely small compared to the K_D values of other globular proteins [approximately 10^{-2} at 42 °C in α-lactalbumin, Takeda et al. (1973); approximately 10^{-6} at 42 °C in lysozyme, Nakanishi et al. (1973)], indicating that the probability of cooperative unfolding is suppressed to an exceptionally low level in the wild-type SSI.

Proteolysis for the Case That $[I]_{total}$ *Is Larger Than* $[E]_{total}$. In order to examine proteolysis of the inhibitor by subtilisin BPN′, either W86H or the wild-type SSI was mixed with smaller amounts of subtilisin BPN′ and aliquots of the mixture were subjected to gel filtration HPLC at appropriate time intervals. Surprisingly, even though the initial ratio of $[E]_{total}/[I]_{total}$ is chosen as 0.39, W86H was found to be digested into peptide fragments in the course of incubation at 42 °C (Figure 9). Under exactly the same conditions, the

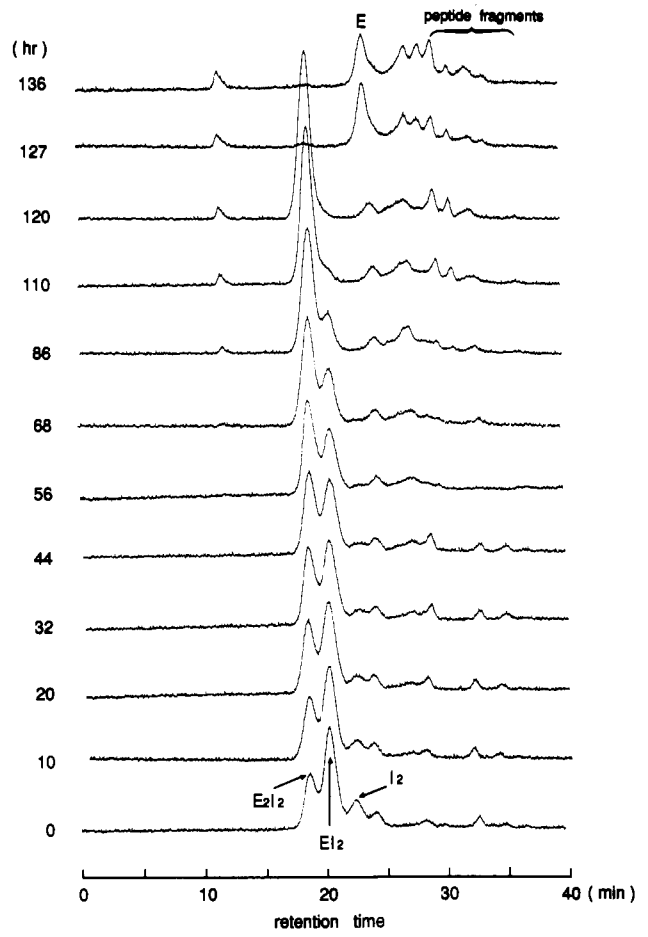

FIGURE 9: Time course of the gel filtration HPLC pattern of a mixture of W86H and subtilisin BPN'. The initial value of α ($=[E]_{total}/[I]_{total}$) was chosen to be 0.39. The mixture was incubated at 42 °C in 0.1 M phosphate buffer (pH 7.0), aliquotes of which were subjected to gel filtration HPLC at appropriate time intervals at 10 °C. Peaks at retention times 18.5, 20.0, and 22.5 min correspond to those of E_2I_2, EI_2, and I_2, respectively.

wild-type SSI underwent practically no changes. In Figure 9, the three peaks with retention times of 18.5, 20.0, and 22.5 min could be assigned unambiguously to E_2I_2 (MW = 78000), EI_2 (50500) and I_2 (23000), respectively. Calculation of the peak intensities revealed that $[E]_{total} = 2[E_2I_2] + [EI_2]$ remained virtually constant and equal to the initial enzyme concentration throughout the incubation period. Therefore, changes in the peak ratios (E_2I_2:EI_2:I_2) were caused only by the reduction of the inhibitor concentration, i.e., by the proteolysis of W86H. This means that the inhibitor W86H was more susceptible to the protease attack than the protease itself. Experimental conditions were carefully chosen to avoid redistribution of the EI_2 into E_2I_2, EI_2, and I_2 throughout the elution period by setting the column temperature at 10 °C at which the rate constant for dissociation of EI into E + I is expected to be smaller than 2.5×10^{-2} min^{-1}, the rate measured at 25 °C by the stopped-flow method (Uehara et al., 1980). The fact that no broadening or reduction of the EI_2 peak was observed throughout the experiment indicates that such redistribution was successfully avoided. On the other hand, a sampling interval of about 10 h at 42 °C was sufficiently long for the enzyme to migrate from one inhibitor molecule to another many times. Therefore, the ratio of the three peaks could be regarded as representing the statistical probability of distribution at each sampling time.

The digestion proceeded in the "all-or-none" fashion; i.e., only the intact inhibitor (complex) and the digested peptide

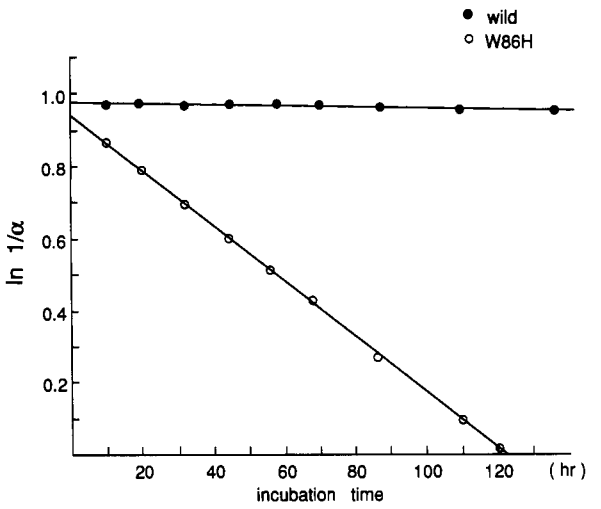

FIGURE 10: Semilogarithmic plot of $1/\alpha$ ($=[I]_{total}/[E]_{total}$) against time of incubation for the wild-type SSI (●) and W86H (○).

fragments were detected. No specific intermediates such as the SSI with the reactive site peptide bond hydrolyzed (SSI*; Hiromi et al., 1985) were detected on HPLC. This does not necessarily deny the formation of SSI* in the initial step of proteolysis. However, even if SSI* were produced, it would form a complex with subtilisin as strongly as SSI does and would not be detected as free SSI* at neutral pH (Hiromi et al., 1985). Free SSI* is known to be formed only at low pH, e.g., pH 2.0, where the SSI and subtilisin are subjected to acid denaturation. Indeed, as is clear from Figure 4, the transition pH for acid denaturation is 3.0 for the wild-type SSI and 4.5 for W86H, far below pH 7.0 at which the present experiment was carried out.

Quantitative Analysis of the HPLC Peaks and Mechanism of the Proteolysis. If we define the ratio $[E]_{total}/[I]_{total}$ to be α, the molar ratio of E_2I_2, and EI_2, and I_2 should be

$$[E_2I_2]:[EI_2]:[I_2] = \alpha^2:[2\alpha(1-\alpha)]:(1-\alpha)^2 \quad (3)$$

from simple statistical consideration, under the conditions that the K_i value is much smaller than the concentrations of I and E and that no cooperativity exists for enzyme binding between the two subunits of I_2, as will be proven later. The molar absorption coefficients of these three species are known to be

$$\epsilon_{E2I2} = 83600 \quad \epsilon_{EI2} = 51200 \quad \epsilon_{I2} = 18700 \quad (M^{-1}\ cm^{-1})$$

for the wild-type SSI (Hiromi et al., 1985). For W86H the absorption coefficients were calculated by considering the lack of Trp86, whose molar absorption coefficient is 5559 M^{-1} cm^{-1} at 280 nm. By multiplying the thus-determined absorption coefficients through eq 3, the ratio of the absorbance A of the HPLC peaks should be

$$A(E_2I_2):A(EI_2):A(I_2) = (\epsilon_{E2I2}\alpha^2):[(\epsilon_{EI2})(2\alpha)(1-\alpha)]:[(\epsilon_{I2})(1-\alpha)^2] \quad (4)$$

The advantage of eq 4 is that only the absorbance ratios are needed for the determination of α ($=[E]_{total}/[I]_{total}$). In practice, as the I_2 peak was superimposed by an impurity peak from subtilisin, the value of α was calculated from the ratio of the two peaks for E_2I_2 and EI_2. This procedure is justified because the ratio of any two of the three peaks is sufficient to determine the value of α uniquely.

No simple relations could be found between the concentration of either E_2I_2, EI_2, or I_2 and the rate of proteolysis. On the other hand, a clear relation was found between $[I]_{total}$ and the rate of proteolysis as shown in Figure 10 where the

semilogarithmic plot of the value $1/\alpha$ ($=[I]_{total}/[E]_{total}$) vs time is shown. Because $[E]_{total}$ ($=2[E_2I_2] + [EI_2]$) was kept constant during the reaction as mentioned earlier, the plots obey first-order kinetics with regard to $[I]_{total}$ with a rate constant of 1.27×10^{-4} min^{-1} at 42 °C (see Table I).

The above observation eliminates the possibility that the digestion reaction occurs exclusively in the EI complex, since in that case the reaction should obey zero-order kinetics because [EI] ($=2[E_2I_2] + [EI_2]$) was constant throughout the experiment. That the EI complex of W86H in the native conformation is stable against the protease attack is reasonable in view of the fact that neither the K_i value nor the conformation around the reactive site in the native state is affected by the mutation. Just as the EI complex of the wild-type SSI is resistant to the proteolysis reaction, so the complexed form of W86H should also be resistant as long as it keeps the same native conformation as the wild type. Thus, in order to explain the mechanism of the proteolysis, we must postulate the existence of an enzyme-susceptible form of the inhibitor (W86H) other than the native conformation.

The fact that a considerable difference in denaturational fluctuation existed between the two inhibitors, as shown by hydrogen–deuterium exchange studies, has led us to postulate that the denatured form of W86H is the enzyme-susceptible form. Even at 42 °C, which is more than 30 deg below T_D, the denaturational fluctuation is significant in W86H. Both the rate of unfolding (k_1) and the equilibrium constant K_D were more than 2 orders of magnitude larger in W86H than in the wild-type SSI, just as the rate of the proteolysis was more than 2 orders of magnitude larger in W86H than in the wild-type SSI (Figure 10). Accordingly, we propose the following mechanism of proteolysis:

$$I \underset{k_2}{\overset{k_1}{\rightleftharpoons}} D \underset{k_4}{\overset{k_3[E]_0}{\rightleftharpoons}} ED \xrightarrow{k_5} E + \text{peptides} \qquad (5)$$

where I is the native form of the inhibitor (W86H) and should include all the forms of I because only $[I]_{total}$ ($=2[E_2I_2] + 2[EI_2] + 2[I_2]$) obeyed first-order kinetics, irrespective of whether I existed in the form of E_2I_2, EI_2, or I_2. D represents the denatured form of W86H which the protease (E) attacks and digests into peptide fragments. Under the condition that $[I]_{total} > [E]_{total}$, the concentration of the free enzyme is infinitesimally small, however, and the proteolysis reaction should be catalyzed by potentially all the bound enzymes in the form of EI (E_2I_2 or EI_2). This would be possible because E is expected to migrate from one I to another I once every few minutes, much more frequently than the denaturational fluctuation. Therefore the rate of binding of E with D can be regarded to be proportional to the total enzyme concentration, which is almost equal to [EI] or the initial enzyme concentration $[E]_0$.

The rate of proteolysis in mechanism 5 can be solved with steady-state approximations for ED and D ($d[ED]/dt = d[D]/dt = 0$) as

$$v = -\frac{d[I]_{total}}{dt} = \frac{k_5 K_D [E]_0}{K_m + (k_5/k_2)[E]_0}[I]_{total} \qquad (6)$$

where $K_D = k_2/k_1$ and K_m [$=(k_4 + k_5)/k_3$] is a Michaelis constant. Equation 6 predicts first-order kinetics as observed.

The notion that the proteolysis reaction proceeds through the denatured form rather than the native form of a protein has been reported in the case of noninhibitor globular proteins (Pace & Barret, 1984; Imoto et al., 1986). This notion has also been used to explain the translocation of polypeptides through biological membranes. In this case, some kind of unfolded state, whether entirely unfolded or having only secondary structure, is protease sensitive and can translocate the membrane, while the folded state which lacks the translocation competence is resistant to proteolysis (Randal & Hardy, 1986; Eilers et al., 1988; Bernstein et al., 1989). The denatured form of W86H seems to be highly sensitive to the protease attack, because the rate of proteolysis ($=1.27 \times 10^{-4}$ min^{-1}) is only 1 or 2 orders of magnitude lower than the rate of unfolding ($=6.3 \times 10^{-3}$ min^{-1}) (see Table I).

The results obtained here indicated that the presence of a significant amount of the unfolded conformation can be lethal for SSI. Even a single amino acid substitution at a position remote from the reactive site can increase such a fluctuation and make the protein vulnerable to protease attack. We may therefore conclude that the molecule of the wild-type SSI has been carefully designed by Nature not only to make its reactive site highly resistant to a protease attack in the native conformation, but also to suppress cooperative fluctuation leading to major unfolding to an extremely low level.

Proteolysis for the Case That $[E]_{total}$ Is Larger Than $[I]_{total}$. Once the concentration of subtilisin ($[E]_{total}$) became larger than the concentration of the mutant SSI ($[I]_{total}$), the rate of proteolysis was accelerated by more than 2 orders of magnitude, as seen in the last three traces (120, 127, and 136 h) of Figure 9. Figure 11 shows the time course of the proteolysis when the initial ratio $[E]_{total}/[I]_{total}$ ($=\alpha$) is 1.0 for W86H as well as for the wild SSI at 42 °C. Here peaks eluting at 18.5 min correspond to E_2I_2 and 24.5 min to E (free enzyme), respectively. The latter peak is superimposed by an impurity peak (degraded form of subtilisin). As the reaction proceeded, the fraction of E_2I_2 decreased gradually with concomitant increase of E. Throughout the reaction, $[I]_{total}$ decreased to almost zero, while the reduction of $[E]_{total}$ was relatively small. This means that the proteolysis of the E_2I_2 complex occurred mainly on the inhibitor and not on subtilisin itself. The site of attack by the free enzyme cannot be the reactive site of the inhibitor, because the inhibitor exists dominantly in the E_2I_2 complex and therefore its reactive site is covered for most of the time with the enzyme molecule. The site of attack must be some portions of the inhibitor molecule exposed to the solvent in the E_2I_2 complex. The first attack will induce successive attacks of the cleaved inhibitor by the enzyme, resulting in the all-or-none type reaction. We note that, under the condition that $[E]_{total}$ was larger than $[I]_{total}$, even the wild-type SSI was digested at a rate comparable with that of W86H. This finding revealed that even the wild-type SSI had not been designed by Nature to work as an inhibitor for the case that the protease is present in excess.

The time courses of the decay of the E_2I_2 peak are plotted in Figure 12, for three initial ratios of $[E]_{total}/[I]_{total}$ ($=\alpha$). The kinetics of proteolysis does not follow a simple first-order reaction, indicating that the mechanism of proteolysis is different from that when excess inhibitor is present. A notable feature of the reaction in Figure 12 is the convergence to first-order kinetics at a later stage of the reaction when the concentration of the free enzyme becomes significant. The first-order rate constants converge to values of 1.34×10^{-2} min^{-1} for the wild-type SSI and 1.87×10^{-2} min^{-1} for W86H irrespective of the initial ratios of $[E]_{total}/[I]_{total}$ chosen (see Table I). The observed rate constants, however, are still smaller by several orders of magnitude than the rate of hydrolysis of small peptide substrates (Fersht, 1984).

Unlike the case when the inhibitor concentration was higher than that of the enzyme, the difference in the rate of proteolysis was quite small between the wild type and W86H. This ob-

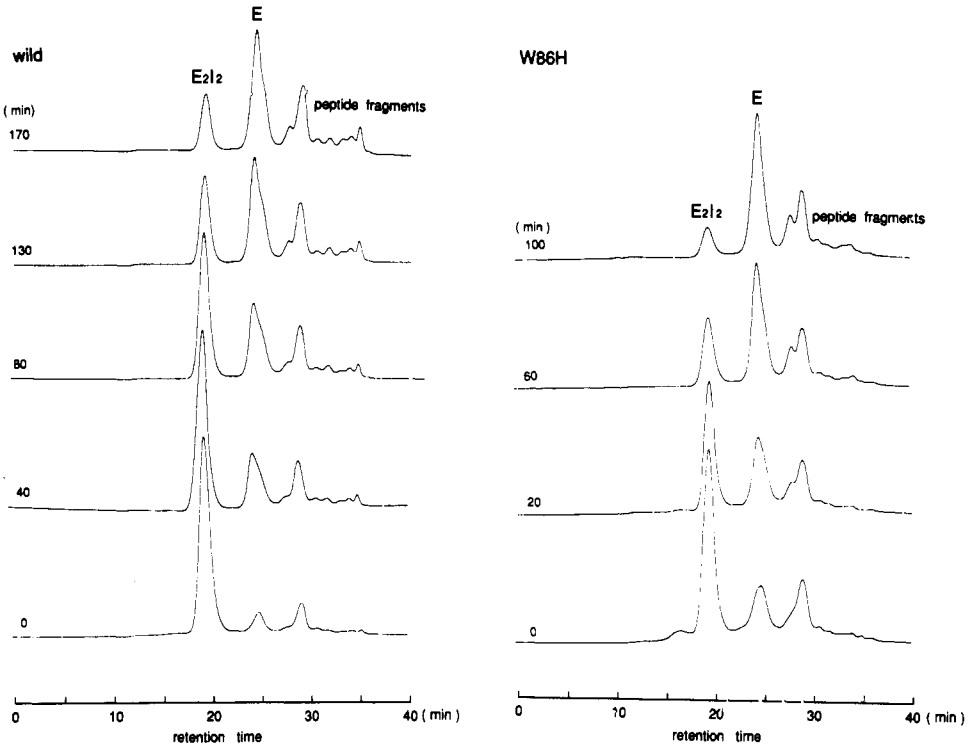

FIGURE 11: Time courses of gel filtration HPLC pattern of a mixture of the wild-type SSI and subtilisin BPN′ (left), and that of a mixture of W86H and subtilisin BPN′ (right), for the initial value of α ($=[E]_{total}/[I]_{total}$) > 1.0. Other conditions were the same as in Figure 9. Peaks at retention times 18.5 and 24.0 min correspond to those of E_2I_2 and free enzyme, respectively.

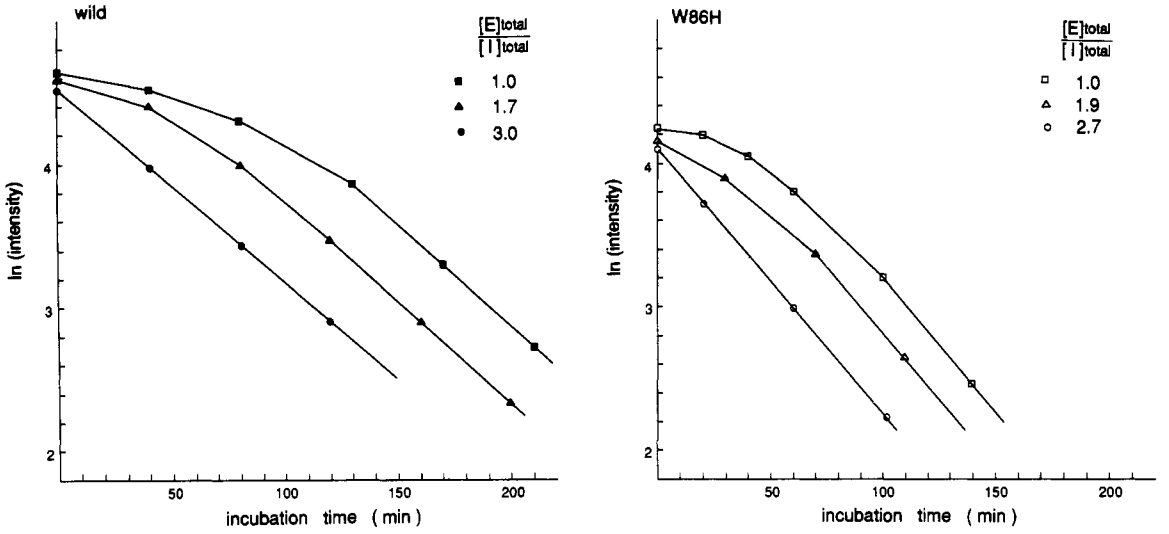

FIGURE 12: Semilogarithmic plots of the HPLC peak intensities of E_2I_2 against time of incubation at 42 °C for the wild-type SSI and for W86H. Initial values of α ($=[E]_{total}/[I]_{total}$) were chosen to be 1.0 (■), 1.7 (▲), and 3.0 (●) for the wild-type SSI and 1.0 (□), 1.9 (△), and 2.7 (○) for W86H.

servation also indicates that the mechanism of the proteolysis is entirely different from the case when $[I]_{total}$ is larger than $[E]_{total}$. The rate constant for the major unfolding of the wild-type SSI in the free form was estimated to be 1.0×10^{-5} min^{-1} at 42 °C from the hydrogen–deuterium exchange experiment. As it is rather difficult to suppose that this rate becomes faster upon complex formation, the rate of the proteolysis of the wild-type SSI (1.34×10^{-2} min^{-1}; see Table I) is estimated to be larger than that of the major unfolding by more than 3 orders of magnitude. Therefore, it is unlikely that the proteolysis reaction proceeds through a cooperative unfolding of the E_2I_2 complex. Instead, we must postulate a more frequent structural fluctuation within the E_2I_2 complex into an enzyme-susceptible form, which may be designated as EI′. We propose the following mechanism of proteolysis for the enzyme excess case, commonly for both the wild-type SSI and W86H:

$$EI \underset{k_2'}{\overset{k_1'}{\rightleftharpoons}} EI' \underset{k_4'}{\overset{k_3'[E]}{\rightleftharpoons}} EI'E \xrightarrow{k_5'} 2E + \text{peptides} \qquad (7)$$

where EI represents the E_2I_2 complex and I′ represents some form of I that is vulnerable to enzyme attack but is not to be identified with the denatured form. This assumption that the E_2I_2 can be digested only when it takes a conformation vulnerable to the enzyme attack enables us to explain the experimentally observed kinetics and especially the approach to the first-order reaction when the concentration of the free enzyme increases. Equation 7 can be solved with the approximation that $[E]_0 = [E] + [EI]$ and under the steady-state condition ($d[EI']/dt = 0$, $d[EI'E]/dt = 0$) as

$$v = -\frac{d[EI]}{dt} = \frac{k_5'K_D'([E]_0 - [EI])[EI]}{K_m' + (k_5'/k_2')([E]_0 - [EI])} \quad (8)$$

where $K_D' = k_1'/k_2'$ and $K_m' = (k_4' + k_5')/k_3'$. Equation 8 can be solved for [EI] and in the case of a large excess of the free enzyme is simplified to

$$\ln [EI] = -k_1't + (\text{constant}) \quad (9)$$

Equation 9 represents the first-order kinetics observed in Figure 12 when excess free enzyme is present. Equation 9 indicates that the experimentally obtained first-order rate constant equals k_1', the rate at which EI takes the EI′ form. The slight difference in k_1' between the wild-type SSI and W86H is attributable to the difference in the rate of fluctuation of EI into EI′. Alternatively, the difference may also be attributable to the coexistence of the unfolded form in W86H, which may slightly accelerate the rate of proteolysis of W86H. The latter possibility cannot be denied even though the unfolding rate is 3 times slower than the rate of proteolysis (see Table I), because the difference in the solvent (^2H_2O and ^1H_2O) for the hydrogen–deuterium exchange and the proteolysis experiments as well as the complex formation somewhat obscure the difference in the rate between the proteolysis and the unfolding.

Although the I′ form cannot be specified at the moment, it should be almost common to the wild-type SSI and W86H, and its formation must be much faster than the major unfolding. One possibility is that the I′ state is related to the dissociation of the dimer structure (E_2I_2) into the monomeric form (2EI). The rate constant for the dissociation of the dimer structure in free SSI is estimated to be slow at 4 °C (Akasaka et al., 1982) but is expected to be of the order of 10^{-1} min^{-1} at 25 °C (Momma and Tonomura, personal communication). Since the I–I interface is maintained by the β-sheets consisting of many hydrophobic amino acids, it appears unlikely that the same conformation of I is maintained when E_2I_2 dissociates into the EI form. All the EI form would immediately transform into EI′, which might be attacked easily by the free enzyme. Such a dissociation should also occur when the inhibitor is present in excess of the enzyme, but would not lead to proteolysis, because no significant concentration of the free enzyme should exist. Another possibility is that the proteolysis proceeds through conformational fluctuations within the E_2I_2 complex (Endo et al., 1985; Fontana et al., 1986).

The mechanism of the proteolysis that operates when the enzyme is in excess should not be effective when the inhibitor is in excess, because in the latter case the enzyme molecules are exclusively trapped by the reactive site of the inhibitor (K_i = 10^{-11}; see Table I). Whatever the details of the mechanism, the results of Figure 12 clearly demonstrate that the wild-type SSI loses its function as an inhibitor as soon as the enzyme concentration increases over that of the inhibitor. This means that the wild-type SSI is designed to operate like a "step function"; i.e., when SSI is produced in excess of the enzyme, it works as a potent inhibitor, and when its concentration declines below that of the enzyme, its function is rapidly lost within a few hours. Whether this is a general design of a proteinaceous protease inhibitor or it is a special case for SSI remains to be clarified in future investigations.

Structural Properties of SSI Essential for Protease Inhibition. Our present study of the mechanism of temporary inhibition of a mutant SSI revealed two characteristic structural properties of SSI, which are essential for being an inhibitor against subtilisin BPN′. These may be put forward as follows.

The first property is that the reactive site is highly resistant to hydrolysis *in the native conformation.* When the wild-type SSI or W86H was present in excess of the protease, the active sites of essentially all the enzyme molecules were occupied by the reactive sites of the inhibitor molecules. In this case, practically no proteolysis reaction occurred. Recent refinement in the X-ray analysis of the SSI–subtilisin BPN′ complex indicates that the carbonyl carbon of Met73 at the reactive site of the wild-type SSI and the Ser Oγ of subtilisin are separated by as much as 2.6 Å, outside the range of nucleophilic attack (Mitsui, private communication). Apparently, this geometry at the interface of the SSI–subtilisin BPN′ complex prevents further reaction to proceed. In contrast, however, when the enzyme is present in excess of the inhibitor, SSI in its native conformation becomes easily susceptible to digestion by subtilisin BPN′. This is because in this case free enzymes can attack peptide bonds other than the reactive site, which are not resistant to protease attack (cf. Figures 11 and 12).

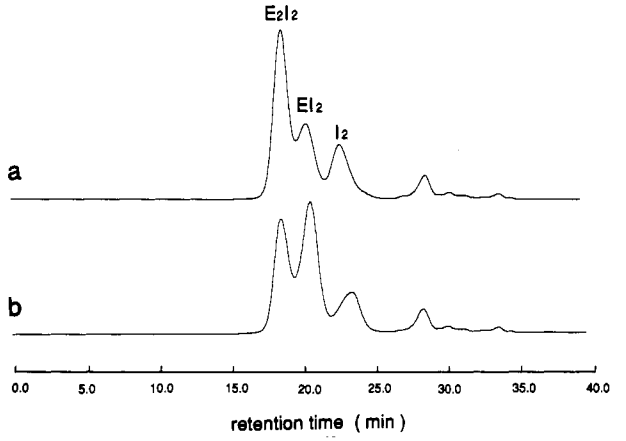

FIGURE 13: Gel filtration HPLC patterns of a mixture of subtilisin BPN′ (E) and the wild-type SSI (I_2) for α (=$[E]_{total}/[I]_{total}$) = 0.50. (a) Immediately after mixing and (b) after sufficient time (2 h) of incubation at 42 °C. Peaks at 18.5, 20.0, and 22.5 min correspond to those of E_2I_2, EI_2, and I_2, respectively.

The second property is that cooperative fluctuations of the molecule that lead to the major unfolding (denaturation) are maintained at an extremely low level in the wild-type SSI (K_D = 5×10^{-10} at 42 °C; see Table I). Impairment of this property by an amino acid substitution, such as Trp86 replaced by His, can increase this level considerably to render SSI vulnerable to the protease attack. The present study has shown that Trp86, filling the gap between the α lobe and the β lobe, is essential for the maintenance of this property. The fact that several other cases of single amino acid replacement in the core region of SSI remote from the reactive site, causing thermodynamic instability of the core, invariably resulted in temporary inhibition (Kojima et al., to be published) has led us to believe that the impairment of this extremely low level of denaturational fluctuation is a general mechanism applicable to most of these cases of temporary inhibition.

Since the tight complex formation between the reactive site of an inhibitor and the active site of an enzyme is general for the interaction betweeen a serine protease and its inhibitor, the first property of SSI should obviously be a general property of serine protease inhibitors. Furthermore, since the rate of proteolysis should intrinsically be rapid when "random coiled" polypeptides are substrates of any serine protease, it would be natural to expect that most serine protease inhibitors, when existing in unfolded states, are susceptible to proteolysis. Thus, the second property of SSI should also be a general property of most serine protease inhibitors. In conclusions, we propose that the two essential structural properties of SSI mentioned above are also two essential structural properties of serine

protease inhibitors in general.

ACKNOWLEDGMENTS

We are indebted to Prof. Takahashi and Dr. Fukada of University of Osaka Prefecture for the DSC measurement on a DASM-4 scanning microcalorimeter and to Dr. Makino and Ms. Hamaguchi of Kyoto Institute of Technology for the use of the HPLC facilities.

APPENDIX

No Cooperativity on Enzyme Binding. Since SSI is a dimeric protein which forms double-headed reactive sites, the equality of the binding ability of these two sites has to be confirmed to ensure eq 3. The binding of the enzyme (subtilisin) to SSI is schematically represented as a two-step reaction:

$$E + I_2 \rightleftharpoons EI_2 \qquad K_1' = \frac{[E][I_2]}{[EI_2]} = 2K_1 \qquad (10)$$

$$E + EI_2 \rightleftharpoons E_2I_2 \qquad K_2' = \frac{[E][EI_2]}{[E_2I_2]} = \frac{K_2}{2} \qquad (11)$$

If no cooperativity exists between the two binding sites, K_1 is equal to K_2. If that is not the case, K_1 and K_2 will be different. Here, as the index for the cooperativity, we define the ratio K_1/K_2 to be β. With the value of β, the molar ratio of E_2I_2, EI_2, and I_2 will be

$$[E_2I_2]:[EI_2]:[I_2] = (\beta\alpha^2):[(1-\alpha)\beta\alpha + (1-\beta\alpha)\alpha]:[(1-\alpha)(1-\beta\alpha)] \qquad (12)$$

by statistical consideration, where α is the ratio $[E]_{total}/[I]_{total}$ as was defined in eq 3. Thus, if the enzyme and the inhibitor solutions are mixed to make a definite molar ratio, e.g., α = 0.5, the value of β will be determined experimentally from the ratio of the two arbitrary peak intensities of the three species such as E_2I_2, EI_2, or I_2. Here the ratio $[E_2I_2]/[EI_2]$ was selected to avoid the superposition of the impurity peak on the I_2 peak. If there were negative cooperativity between the two binding sites of SSI, i.e., if the enzyme bound, the value of β would be smaller than 1. On the other hand, if there was no cooperativity, the value of β would be 1.

Figure 13 shows the results of the mixing of the wild-type SSI and subtilisin BPN′ in the ratio α = 0.5 before incubation (a) and after sufficient time (2 h) for incubation at 42 °C (b). The concentration of SSI was measured by UV absorption, and that of subtilisin BPN′ was determined by using the standard SSI solution (Tonomura et al., personal communication). From the experimental ratio of $[E_2I_2]/[EI_2]$ of Figure 13b, the value of β was determined to be 1.04, close to the theoretical value of 1.0 for the noncooperative case. This indicates that there is no cooperativity between the two enzyme binding sites, i.e., $K_1 = K_2$. If $K_1' = 2K_1 = 0.5 \times 10^{-9}$ (M) and $K_2' = K_2/2 = 9.4 \times 10^{-9}$ (M) as Kano et al. (1983) reported, the value β should be only 0.0133. If this were the case, the ratio $[E_2I_2]/[EI_2]$ would be 0.0066 and the E_2I_2 peak would be undetectable.

REFERENCES

Akasaka, K., Fujii, S., & Kaptein, R. (1981) *J. Biochem. 89*, 1945–1949.

Akasaka, K., Fujii, S., Hayashi, F., Rokushika, S., & Hatano, H. (1982) *Biochem. Int. 5*, 637–642.

Akasaka, K., Inoue, T., Hatano, H., & Woodward, C. (1985) *Biochemistry 24*, 2973–2979.

Akasaka, K., Inoue, T., Tamura, A., Watari, H., Abe, K., & Kainosho, M. (1988) *Proteins: Struct., Funct., Genet. 4*, 131–136.

Aoshima, H. (1976) *Biochim. Biophys. Acta 453*, 139–150.

Bernstein, H. D., Rapoport, T. A., & Walter, P. (1989) *Cell 58*, 1017–1019.

Coplen, L. J., Frieden, R. W., & Goldenberg, D. P. (1990) *Proteins: Struct., Funct., Genet. 7*, 16–31.

Eilers, M., Hwang, S., & Schatz, G. (1988) *EMBO J. 7*, 1139–1145.

Eisenberg, D., & McLachlan, A. D. (1986) *Nature 319*, 199–203.

Endo, S., Nagayama, K., & Wada, A. (1985) *J. Biomol. Struct. Dyn. 3*, 409–421.

Fersht, A. (1984) *Enzyme Structure and Mechanism*, Freeman, San Francisco.

Fontana, A., Fassina, G., Vita, C., Dalzoppo, D., Zamai, M., & Zambonin, M. (1986) *Biochemistry 25*, 1847–1851.

Fujii, S., Akasaka, K., & Hatano, H. (1980) *J. Biochem. 88*, 789–796.

Fujii, S., Akasaka, K., & Hatano, H. (1981) *Biochemistry 20*, 518–523.

Gross, K., & Kalbitzer, H. R. (1988) *J. Magn. Reson. 76*, 87–99.

Harada, I., Takeuchi, H., Tasumi, M., Tsuji, T., & Kainosho, M. (1982) *J. Raman Spectrosc. 13*, 276–279.

Hiromi, K., Akasaka, K., Mitsui, Y., Tonomura, B., & Murao, S. (1985) *Protein Protease Inhibitor—The case of Streptomyces Subtilisin Inhibitor*, Elsevier, Amsterdam.

Hirono, S., Akagawa, H., Mitsui, Y., & Iitaka, Y. (1984) *J. Mol. Biol. 178*, 389–413.

Hvidt, A., & Nielsen, S. O. (1966) *Adv. Protein Chem. 21*, 287–386.

Imoto, T., Yamada, H., & Ueda, T. (1986) *J. Mol. Biol. 190*, 647–649.

Inouye, K., Tonomura, B., Hiromi, K., Sato, S., & Murao, S. (1977) *J. Biochem. 82*, 1207–1215.

Kano, K., Ikeda, T., & Senda, M. (1983) *Agric. Biol. Chem. 47*, 559–563.

Katz, E., Thompson, C. J., & Hopwood, D. A. (1983) *J. Gen. Microbiol. 129*, 2703–2714.

Koide, T., Ikenaka, T., Ikeda, K., & Hamaguchi, K. (1974) *J. Biochem. 75*, 805–823.

Kojima, S., Obata, S., Kumagai, I., & Miura, K. (1990) *Bio/Technology 8*, 449–452.

Komiyama, T., & Miwa, M. (1980) *J. Biochem. 87*, 1029–1036.

Komiyama, T., Miwa, M., Yatabe, T., & Ikeda, H. (1984) *J. Biochem. 95*, 1569–1575.

Kress, L. F., Wilson, K. A., & Laskowski, M., Sr. (1968) *J. Biol. Chem. 243*, 1758–1762.

Mitsui, Y., Satow, Y., Watanabe, Y., & Iitaka, Y. (1979a) *J. Mol. Biol. 131*, 697–724.

Mitsui, Y., Satow, Y., Watanabe, Y., Hirono, S., & Iitaka, Y. (1979b) *Nature 277*, 447–452.

Momma, K., Tonomura, B., Nirasawa, T., Kainosho, M., Tamura, A., Kanaori, K., Akasaka, K., Kojima, S., Kumagai, I., & Miura, K. (1990) *Nippon Nougeikagaku Kaishi 64*, 453 (in Japanese).

Morinaga, Y., Franceschini, T., Inouye, S., & Inouye, M. (1984) *Bio/Technology 2*, 636–639.

Nakanishi, M., & Tsuboi, M. (1976) *Biochim. Biophys. Acta 434*, 365–376.

Nakanishi, M., Tsuboi, M., & Ikegami, A. (1973) *J. Mol. Biol. 75*, 673–682.

Nozaki, Y., & Tanford, C. (1971) *J. Mol. Biol. 246*, 2211-2217.
Obata, S., Taguchi, S., Kunagai, I., & Miura, K. (1989a) *J. Biochem. 105*, 367-371.
Obata, S., Furukubo, S., Kumagai, I., Takahashi, H., & Miura, K. (1989b) *J. Biochem. 105*, 372-376.
Odani, S., & Ikenaka, T. (1978) *J. Biochem. 83*, 747-753.
Pace, C. N., & Barrett, A. J. (1984) *Biochem. J. 219*, 411-417.
Privalov, P. L. (1979) *Adv. Protein Chem. 33*, 167-241.
Privalov, P. L. (1989) *Annu. Rev. Biophys. Biophys. Chem. 8*, 47-69.
Privalov, P. L., & Gill, S. J. (1988) *Adv. Protein Chem. 39*, 191-234.
Randal, L. L. & Hardy, S. J. S. (1986) *Cell 46*, 921-928.
Sakai, M., Odani, S., & Ikenaka, T. (1980) *J. Biochem. 87*, 891-898.
Sato, S., & Murao, S. (1973) *Agric. Biol. Chem. 37*, 1067-1074.
Schechter, I., & Berger, A. (1967) *Biochem. Biophys. Res. Commun. 27*, 157-162
Takahashi, K., & Sturtevant, J. M. (1981) *Biochemistry 20*, 6185-6190.
Takahashi, T., Nakanishi, M., & Tsuboi, M. (1978) *Bull. Chem. Soc. Jpn. 51*, 1988-1990.
Takesada, H., Nakanishi, M., & Tsuboi, M. (1973) *J. Mol. Biol. 77*, 605-614.
Tsuboi, M., & Nakanishi, M. (1979) *Adv. Biophys. 12*, 101-130.
Uehara, Y., Tonomura, B., & Hiromi, K. (1980) *Arch. Biochem. Biophys. 202*, 250-258.
Westler, W. M., Kainosho, M., Nagao, H., Tomonaga, N., & Markley, J. L. (1988) *J. Am. Chem. Soc. 110*, 4093-4095.
Woodward, C., Simon, I., & Tuechsen, E. (1982) *Mol. Cell. Biochem. 48*, 135-160.
Wüthrich, K. (1986) *NMR of Proteins and Nucleic Acids*, John Wiley & Sons, New York.

Aspartic Acid Residues at Positions 190 and 192 of Rat DNA Polymerase β Are Involved in Primer Binding†

Takayasu Date,*,‡ Setsuko Yamamoto,‡ Kiyomi Tanihara,‡ Yoshio Nishimoto,§ and Akio Matsukage§
Department of Biochemistry, Kanazawa Medical University, Uchinada-cho, Ishikawa-ken 920-02, Japan, and Laboratory of Cell Biology, Aichi Cancer Center Research Institute, Chikusa-ku, Nagoya 464, Japan
Received September 26, 1990; Revised Manuscript Received March 1, 1991

ABSTRACT: The sequence Gly-Asp-Met-Asp, spanning positions 189–192 of rat DNA polymerase β, is similar to the sequence motif Gly-Asp-Thr-Asp that is highly conserved in a number of replicative DNA polymerases from eukaryotic cells, viruses, and phages. The role of this sequence in the catalytic function of rat DNA polymerase β was investigated by individually changing each amino acid in this region by site-directed mutagenesis. The mutant enzymes DE190 and DE192, in which aspartic acid residues at positions 190 and 192, respectively, were replaced by glutamic acid, showed about 0.1% activity of the wild-type enzyme. On the other hand, the replacement of Gly-189 by alanine or Met-191 by isoleucine or threonine only slightly affected the enzyme activity. A gel mobility shift assay showed that DNA complexes with enzyme DE190 and especially with DE192 were less stable than the corresponding complex with the wild-type enzyme. Kinetic analysis with these mutant enzymes indicate that their K_m's for primer DNA were about 10-fold higher than that of the wild type, while K_m's for deoxyribonucleoside triphosphate were not changed. Since neither DE190 nor DE192 had any significant alteration in secondary structure, our results suggest that both Asp-190 and Asp-192 are located in the active site and are involved in the interaction of DNA polymerase β with primer.

DNA polymerase β is found in a wide range of animals, from sponges to humans but not in plants or bacteria (Chang, 1976), and is believed to function in DNA repair (Friedberg, 1985) and in DNA recombination (Hirose et al., 1989). The enzyme consists of a single polypeptide of approximately 38 kDa[1] and is the smallest among known prokaryotic and eukaryotic DNA polymerases. The amino acid sequence of DNA polymerase β in various vertebrates is highly conserved (Fry & Loeb, 1986); the enzymes from rat and human are composed of 335 amino acids (including a methionine at the N terminus) deduced from cDNA and genomic nucleotide sequences (Zmudzka et al., 1986; Matsukage et al., 1987; SenGupta et al., 1986). An active recombinant rat DNA polymerase β has been overproduced in *Escherichia coli* and purified to homogeneity (Date et al., 1988).

The localization of different functional regions in rat DNA polymerase β has been suggested. The template DNA-binding acivity has been proposed to reside in the N-terminal 20% of this enzyme (Kumar et al., 1990a,b). A lysine residue at position 71 is proposed to be located in or around the nucleotide-binding pocket, since pyridoxal 5′-phosphate covalently bound to this residue inhibited the deoxyribonucleoside triphosphate binding (Basu et al., 1989). Additionally, site-directed mutagenesis indicated that Arg-183 is involved in

† This work was supported in part by a grant from the Foundation for Promotion of Cancer Research backed by the Japan Shipbuilding Industry Foundation to T.D. and by grants-in-aid for Scientific Research from the Japanese Ministry of Education, Science, and Culture to A.M.
* Corresponding author.
‡ Kanazawa Medical University.
§ Aichi Cancer Center Research Institute.

[1] Abbreviations: bp, base pair(s); kDa, kilodalton; IPTG, isopropyl β-D-thiogalactopyranoside; CD, circular dichroism.

0006-2960/91/0430-5286$02.50/0